TECTONOPHYSICS

Tectonophysics 334 (2001) 77–99

www.elsevier.com/locate/tecto

Thermal history of Tertiary basins in Slovenia (Alpine–Dinaride–Pannonian junction)

Reinhard F. Sachsenhofer[a,*], Bogomir Jelen[b], Christian Hasenhüttl[a], István Dunkl[c,d], Thomas Rainer[a]

[a]*Institut für Geowissenschaften, Montanuniversität Leoben, Peter-Tunner-Strasse 5 A-8700 Leoben, Austria*
[b]*Geološki zavod Slovenije, Dimiceva 14, SI-1000 Ljubljana, Slovenia*
[c]*Institut für Geologie und Paläontologie, Universität Tübingen, Sigwartstraße 10, D-72076 Tübingen, Germany*
[d]*Laboratory for Geochemical Research, Hungarian Academy of Sciences, Budapest, Hungary*

Accepted 27 February 2001

Abstract

The transition zone between the Alps, the Dinarides, and the Pannonian Basin was affected by syn-collisional magmatism in Oligocene time and post-collisional lateral escape followed by extreme extension in early and middle Miocene times. Numeric heat flow models for sixteen sites and 650 vitrinite reflectance data from Paleogene and Neogene sediments were used to evaluate temporal and lateral heat flow variations related to these events.

Oligocene. Oligocene (Smrekovec) volcanism is the main heat source for Paleogene sediments south of the Periadriatic Lineament. Vitrinite reflectance patterns suggest dextral displacement along the Donat Fault of the order of 50 km. Coalification of Paleogene coal-bearing sequences south of the Pohorje is a result of the emplacement of the Oligocene Pohorje tonalite.

Early/middle Miocene. Extremely elevated early/middle Miocene heat flow (>200 mW/m^2) occurred in the Styrian Basin, the Pohorje area, the Maribor–Radgona area, and along the Boč Anticline. It is partly a consequence of magmatic activity. However, no igneous rocks are known from the Maribor–Radgona area. A large shallow early Miocene pluton could explain the observed Miocene heat flow. Rapid uplift of hot basement rocks in the Pohorje/Kozjak region may have increased surface heat flow. Neither volcanic rocks nor metamorphic core complexes are known from the Boč area. The Ormož–Selnica Anticline was probably influenced by a middle Miocene heating event (~150 mW/m^2). Coeval volcanism south of the anticline represents a potential heat source.

Post-middle Miocene. The WSW–ENE-trending Ljutomer and Radgona Depressions are characterized by moderate Neogene heat flow (60–75 mW/m^2), whereas late Miocene to present-day heat flow in the Ormož–Selnica Anticline is 80–90 mW/m^2. A recent heat flow anomaly occurs in the Šomat-Benedikt area.

Keywords: post-collisional history; heat flow; Eastern Alps; Pannonian Basin; Dinarides

1. Introduction

The Alps, the Dinarides, and the Carpathians fringe the Tertiary Pannonian Basin (Fig. 1). Research on the Alpine–Carpathian–Pannonian system intensified during the past decades and resulted in many new ideas on its evolution (e.g. Royden and Horváth, 1988; Horváth, 1993). Basin formation in the Pannonian realm started during Paleogene time. Tari et al. (1993) suggest that Paleogene sediments were deposited in retro-arc flexural basins. The Neogene to

* Corresponding author. Fax: +43-384-240-2902.
E-mail address: sachsenh@unileoben.ac.at (R.F. Sachsenhofer).

0040-1951/01/$ - see front matter
PII: S0040-1951(01)00057-9

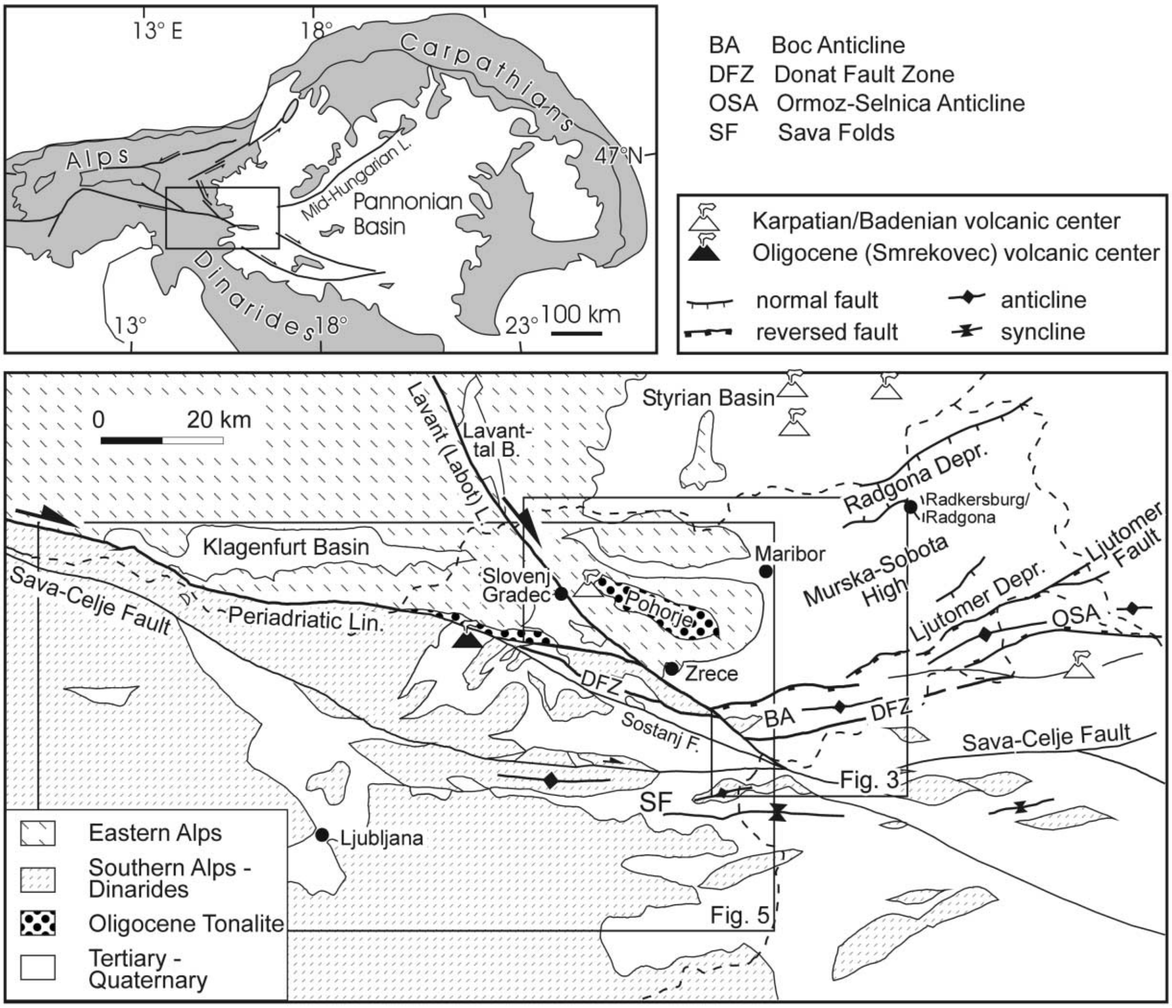

Fig. 1. Location of the study area within the Alpine–Carpathian–Pannonian system. Tectonic sketch map simplified after Fodor et al. (1998).

Quaternary evolution of the Pannonian realm is subdivided into four periods (Tari and Horváth, 1995): early Miocene continental escape of the Eastern Alps, middle Miocene syn-rift extension, late Miocene to Pliocene post-rift extension, and Quaternary neotectonics.

There is a close interrelationship between geodynamics and the thermal evolution of the lithosphere. This is because heat flow is not only a result of tectonic processes, but influences their mode as well (e.g. Buck, 1991). In recent years considerable progress has been made in understanding the relationship between lithosphere rheology and basin evolution in the Pannonian realm (for a summary see Lankreijer, 1998). However, these studies also have shown the need for additional thermal investigations, which provide fundamental constraints on thermomechanical models of the lithosphere.

In the present paper we study the thermal evolution of Paleogene and Neogene sedimentary basins in the transition zone between Eastern Alps, Southern Alps–Dinarides, and the Pannonian Basin. This region is a key area for the understanding of the Pannonian realm. This is because the border between Eastern Alps and Southern Alps, the Periadriatic Lineament, played a major role during early Miocene continental escape (e.g. Kázmér and Kovács, 1985; Ratschbacher et al., 1991; Csontos et al., 1992; Fodor et al., 1998; Frisch et al., 1998) and because the Alpine–Pannonian transition zone is characterized by extreme middle Miocene extension resulting in the formation of deep basins (e.g. Styrian Basin), and the exhumation of metamorphic core complexes (Tari et al., 1999; Frisch et al., 2000). Lateral movements of the order of several hundred kilometers along the Periadriatic Lineament (e.g. Kázmér, 1984; Tari et al., 1995), Oligocene and Miocene magmatic events (e.g. Faninger, 1970), and significant Neogene block rotations (Fodor et al., 1998) provide further evidence for high mobility of the transition zone.

Because of the sensitive reaction of organic matter to increasing temperatures, the thermal history of sedimentary basins can be deduced from maturation studies. The most widely used rank parameter is vitrinite reflectance. In the first part of the paper we present vitrinite reflectance maps of outcropping Paleogene and Neogene sediments and reflectance curves of wells. In the second part, fission-track geochronology and numeric models are used to reconstruct heat flow histories. Special emphasis is put on temporal and lateral heat flow variations. Vitrinite reflectance patterns are also used to estimate the amounts of lateral and vertical movements along major tectonic lines.

Because hydrocarbon generation is controlled by the thermal history of potential source rocks, the relevance of the present study lies not only in providing constraints on basin formation models, but also in the information it provides on hydrocarbon generation in the western Pannonian Basin, which is an active exploration area (e.g. Barić et al., 1996; Hasenhüttl et al., 2001).

2. Geological setting

The Eastern Alps–Southern Alps–Dinarides–Pannonian Basin junction area is characterized by WNW–ESE- to E–W-trending, right-lateral shear zones (Premru, 1976, 1981; Fodor et al., 1998; see Fig. 1 for details). Major faults are the Periadriatic Lineament separating Austroalpine from Southern Alpine basement rocks and the Donat Fault zone. Both tectonic lines were displaced in late Miocene/Pliocene time by the dextral Labot (Lavanttal) Line (Kázmér et al., 1996). The eastern continuation of the Periadriatic Lineament is still a matter of controversy. However, there is evidence that it continues into the WSW–ENE-striking Ljutomer Fault and the mid-Hungarian Line (e.g. Poljak, 1984; Plenič ar et al., 1990; Tari et al., 1995; Fodor et al., 1998; Fig. 1). The tectonic lines separate areas with markedly different Paleogene to early Miocene histories (Jelen et al., 1992; Fig. 2).

Miocene sedimentation north of the Donat Fault began during the late early Miocene (Karpatian; for local Paratethys stages see Fig. 2). Small remnants of Paleocene and middle Eocene sediments are preserved north of the Periadriatic Lineament (Hamrla, 1988), and upper Eocene coal-bearing and carbonaceous sediments (Jelen et al., 1998a,b) occur between the Periadriatic Lineament and the Donat Fault zone. Oligocene magmatism produced tonalites (e.g. in the Pohorje, Fig. 1), which are genetically related to a belt of calc-alkaline plutons along the Periadriatic Lineament (Exner, 1976; Laubscher, 1983; von Blankenburg and Davies, 1995). Early/middle Miocene (~17–15 Ma) latitic rocks are widespread in the Styrian Basin (Ebner and Sachsenhofer, 1995; Harangi et al., 1995), and dacites of roughly the same age occur in the western Pohorje (Faninger, 1970; Fig. 1).

Sedimentation south of the Donat Fault started during the latest Eocene (Jelen et al., 1998a,b) and continued into the early Miocene (Fig. 2). Coal seams, andesites and andesitic tuffs occur within the more than 1000-m-thick sequence. A center of Oligocene (~32–25 Ma) volcanism was located in the Smrekovec area (Odin et al., 1994; Jelen et al., 1998a,b). A major unconformity separates Oligo-/Miocene from middle Miocene to Pliocene sediments. Middle Miocene (~15–13 Ma) volcanic rocks occur in the eastern study area (Pamić and Pécskay, 1996; Fig. 1).

The area east of Maribor is dominated by WSW–ENE-trending fault-bounded troughs separated by a basement high (Durasek, 1991; Fig. 1). The Ljutomer Fault, a normal fault that was reactivated during post-Miocene times as a reverse fault (Durasek, 1991; Horváth, 1995), separates the southern trough, filled with more than 5-km-thick Neogene sediments, from a transpressional zone with WSW–ENE-trending

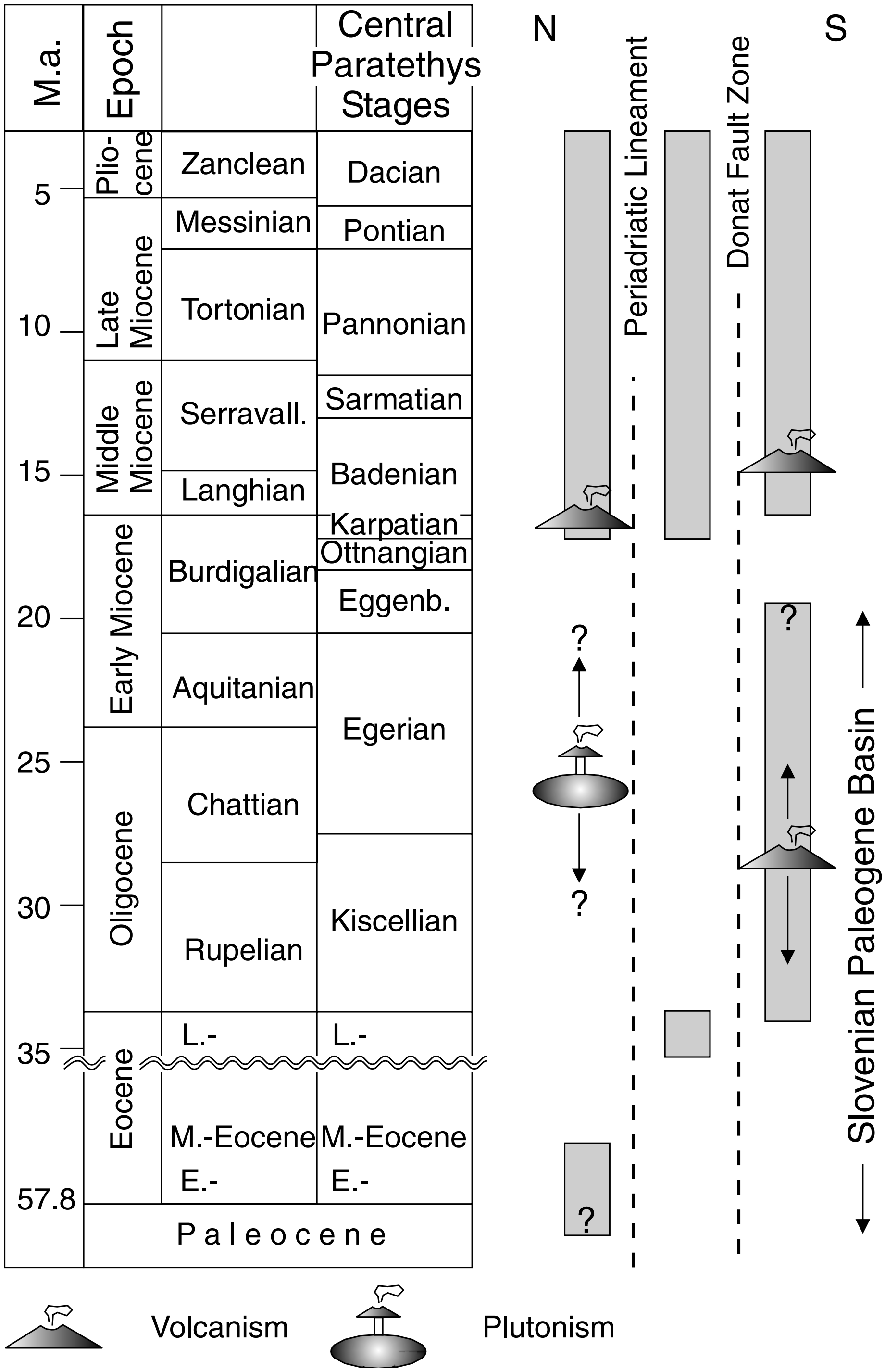

Fig. 2. Oligocene–Miocene correlation of Central Paratethyan stages to the standard time-scale (according to Rögl, 1996) and stratigraphic range of sediments in the study area. The timing of magmatic events is indicated.

anticlines (Boč and Ormož-Selnica anticlines). The latter formed by inversion of early/middle Miocene halfgrabens (Pogácsás et al., 1994; Horváth, 1995). The most uplifted part of the anticlines is Mt. Boč, built up by Permo-Mesozoic carbonates that overthrust Miocene sediments along their northern margin (Winkler-Hermaden, 1957). Vertically dipping late Miocene sediments are evidence for the young age of basin inversion. Basin inversion and the formation of anticlines is caused by counterclockwise rotation of crustal blocks north of the Ljutomer Fault and by dextral movements along the Labot Line (Fodor et al., 1998). The tectonic style of the southern study area is dominated by E–W-striking synclines and anticlines (Sava Folds). Pre-Tertiary rocks and their Oligocene cover are exposed along anticlines, Neogene sediments are preserved in synclines.

3. Methods

About 550 fine-grained and/or coaly sediments were taken from outcrops and boreholes in the frame of an Austrian/Slovenian project. Vitrinite reflectance of these sediments was measured following established procedures (Taylor et al., 1998). Results are presented as mean random reflectance values (Rr). Information on vitrinite reflectance of about 100 additional samples was taken from literature (Hamrla, 1985/86, 1988, 1989; Jelen, 1985/86; Laczó and Jámbor, 1988; Sachsenhofer, 1992).

Isomerisation of biomarker molecules (e.g. Mackenzie, 1984) is an independent rank parameter and can be used to calibrate numeric heat flow models. For the present study, biomarker ratios (20S/[20S + 20R] steranes, 22S/[22S + 22R] hopanes) were provided by the Institute for Petroleum and Organic Geochemistry (ICG-4), KFA Jülich, Germany.

Apatite fission-track geochronology was done to determine the age constraints of the final cooling of the thermally overprinted Neogene sediments. The experimental procedure is described in Sachsenhofer et al. (1998b).

Basin modeling is a standard technique for the reconstruction of paleo-heat flow (Yalçin et al., 1997). PDI-1D™ software of IES, Jülich (Wygrala, 1988) was used to model the thermal histories of 15 wells. Input data include the thickness of distinct stratigraphic units (events), the physical properties of their lithologies and heat flows for each event, as well as the temperature at the sediment-water interface at the time of deposition. Predefined physical parameters for different lithologies are offered by the PDI-1D™ software. These values were modified to account for average depth–porosity trends and thermal conductivities of psammitic and pelitic rocks in the Pannonian Basin (Dövényi and Horváth, 1988; Table 1). The reconstructed heat flow histories were calibrated with recent formation temperatures (Ravnik, 1991), vitrinite reflectance data and biomarker ratios (sterane- and hopane-isomerization). Calculation of vitrinite reflectance followed the kinetic "Easy%Ro" approach of Sweeney and Burnham (1990). Biomarker ratios were calculated using kinetic data of Mackenzie and McKenzie (1983).

4. Vitrinite reflectance patterns

Vitrinite reflectance of Cenozoic sediments along the southeastern margin of the Alps is summarized in Fig. 3 together with reflectance trends of some wells. Vitrinite reflectance curves of additional wells are presented in Fig. 4. Fig. 5 shows isoreflectivity lines for Paleogene sediments in the western part of the study area. The maturity patterns are described separately for regions that are bordered by major tectonic lines.

4.1. Sedimentary Basins north of Periadriatic Lineament–Ljutomer Fault

South(west)ern margin of Pohorje Mountain. Early Miocene (Karpatian) sediments are exposed between the Periadriatic Lineament and the Labot Line south of Slovenj Gradec (Fig. 3). Their vitrinite reflectance increases from the southern and western margins of the basin (0.3–0.5%Rr) towards the Labot Line and reaches maximum values (0.78%Rr) in erosional relics resting on pre-Tertiary basement rocks.

Near Zreče, mature coal-bearing upper Cretaceous to Eocene sediments (0.65–0.8%Rr; Fig. 3) are unconformably overlain by early Miocene (Karpatian) deposits with significantly lower maturity (0.41–0.52%Rr). A plot of vitrinite reflectance versus depth was constructed using information from several

Table 1
Physical properties assigned to standard and user defined (*) lithotypes used for simulations. Permeabilities (−5 means 10^{-5} md) are calculated for different stages of porosity

Lithotype	Density (kg/m^3)	Initial porosity	Compress (Pa^{-1})		Matrix thermal conductivity (W/m K)		Heat capacity (cal/g) K		Permeability at porosity of	
			Max.	Min.	0°C	100°C	20°C	100°C	5%	75%
Water	1160	0	2	1	0.60	0.68	0.999	1.008	1.0	1.0
Sandstone	2660	42	500	10	3.12	2.64	0.178	0.209	−2.0	0.0
Shal & Sand	2669	52	2800	10	2.65	2.38	0.197	0.236	-4.0	3.0
Shale, sandy	2674	57	9000	10	2.32	2.12	0.205	0.248	−4.5	0.0
Shale, tuff	2675	60	15000	10	2.21	2.10	0.205	0.248	−5.5	−1.0
Limestone	2710	42	300	25	2.83	2.56	0.195	0.223	−4.0	13.0
Lime, marly	2707	46	500	20	2.63	2.41	0.201	0.235	−4.5	6.0
*Marl 0%	2610	52	500	35	4.00	3.42	0.178	0.209	−2.0	0.0
*Marl 30%	2604	56	850	35	3.49	3.07	0.187	0.221	−4.0	0.0
*Marl 50%	2600	59	1100	38	3.22	2.87	0.193	0.229	−4.0	3.0
*Marl 70%	2596	61	1400	42	2.99	2.69	0.199	0.236	−4.5	0.0
*Marl 100%	2590	65	2000	50	2.70	2.47	0.208	0.248	−5.0	−1.0
*calc. Shale	2681	55	7000	10	2.27	2.11	0.206	0.248	−3.5	4.25
Basement	2750	5	2	1	2.72	2.35	0.188	0.223	−16.0	−16.0

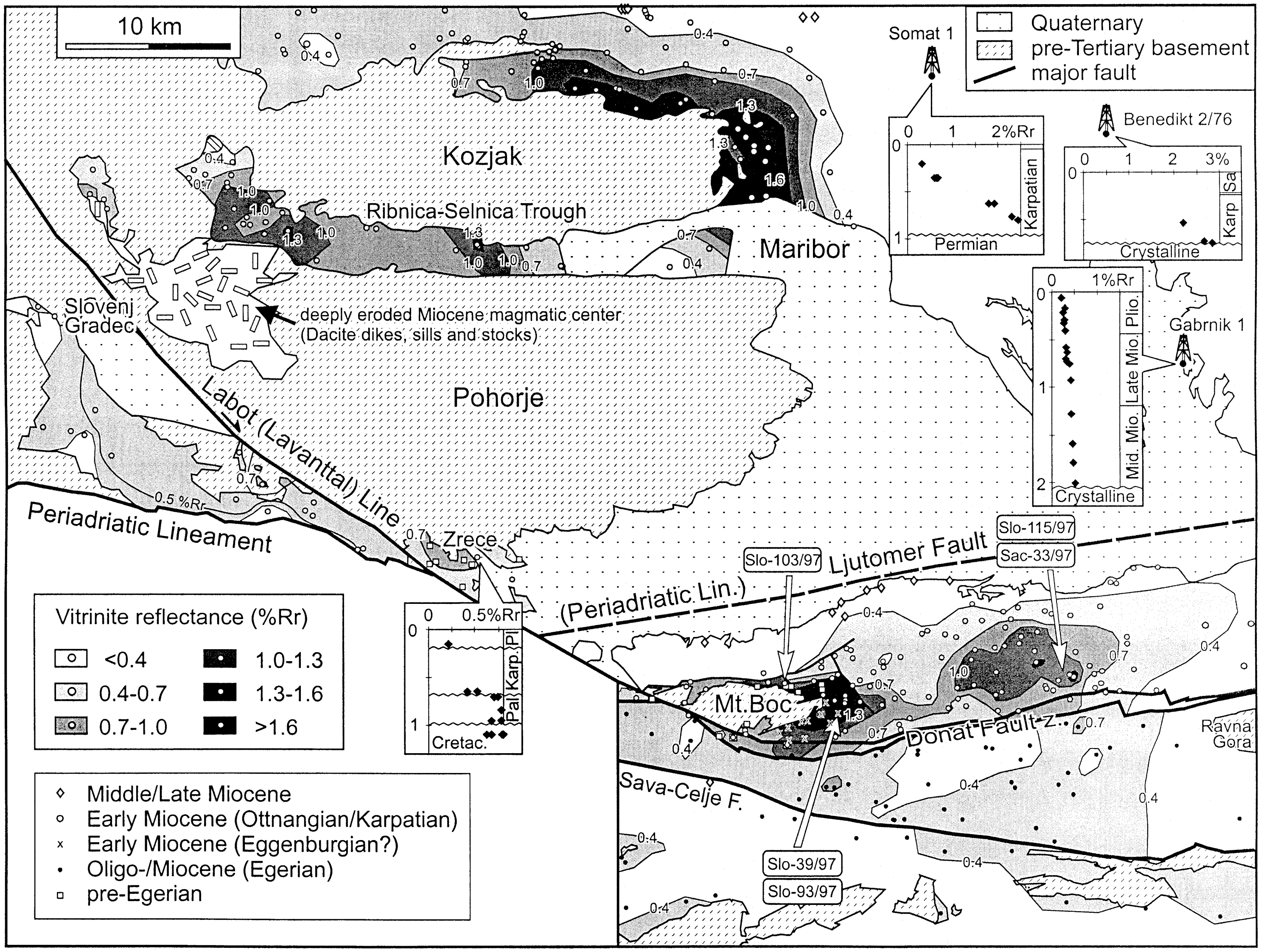

Fig. 3. Vitrinite reflectance map of Cenozoic sediments at the eastern margin of the Alps (see Fig. 1 for location of map). The stratigraphic age of studied samples is indicated by symbols. Inserts show vitrinite reflectance profiles for wells Šomat 1, Benedikt 2/76, Gabrnik 1, and the Zreče area (Sachsenhofer 1998a; Jelen, 1985/86; Hamrla, 1988). The location of fission-track samples Sac-33/97, Slo-39/97, Slo-93/97, Slo-103/97 and Slo-115/97 is shown.

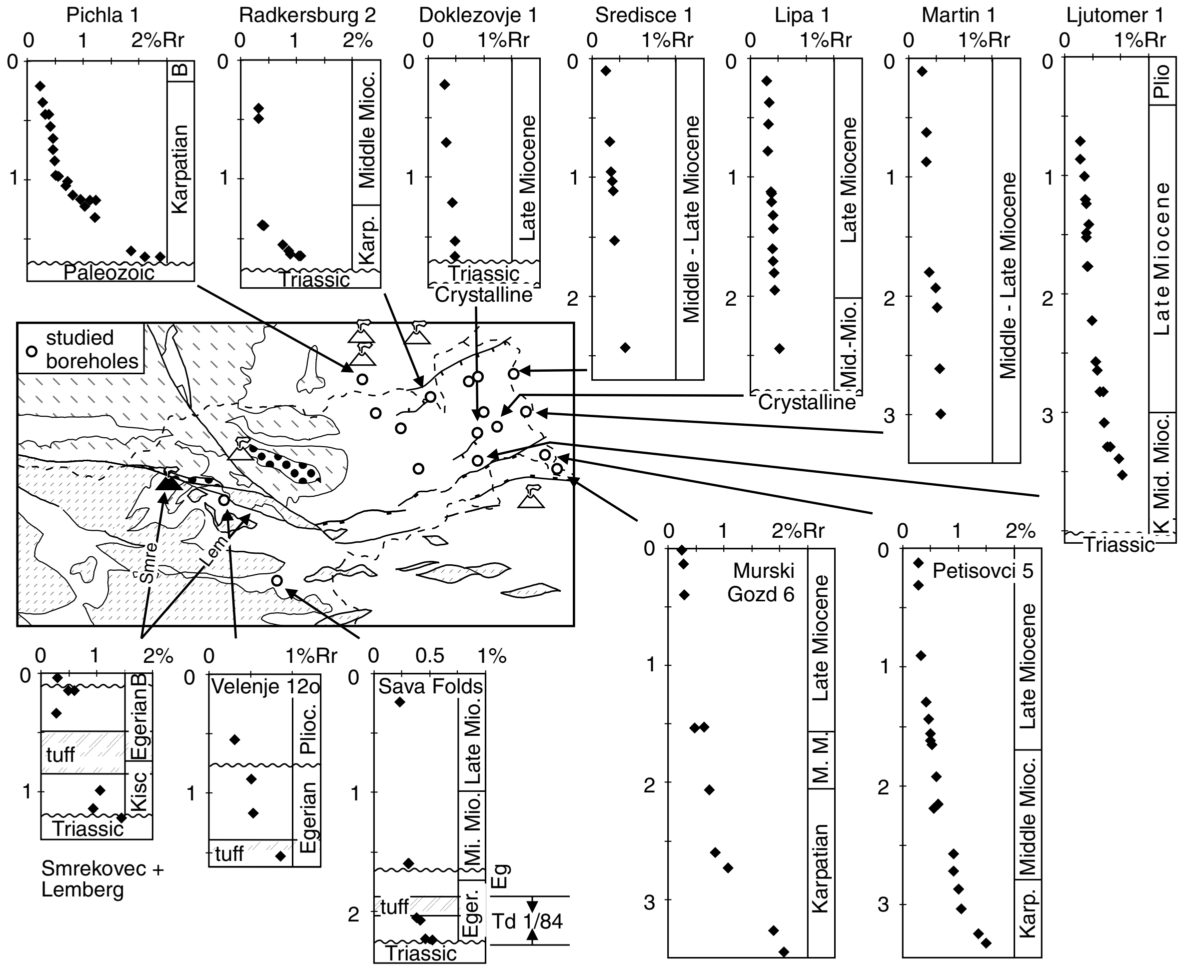

Fig. 4. Position of studied boreholes and vitrinite reflectance profiles for selected wells and surface sections. In addition to new data, vitrinite reflectance values from the following publications have been used: Hamrla (1989); Sachsenhofer (1992). Stratigraphic information is from the above authors, Rijavec (1976), Brezigar et al. (1987), Petrica et al. (1995), and unpublished reports. Wavy lines represent major unconformities.

wells (Hamrla, 1988). It shows a break in vitrinite reflectance between Paleogene and Neogene sediments (Fig. 3). Although the original thickness of the upper Cretaceous to Paleogene sequence was almost 500 m, there is essentially no increase in vitrinite reflectance with age.

Maribor–Radgona area. Vitrinite reflectance of outcropping early Miocene (Ottnangian/Karpatian) sediments in the Ribnica–Selnica Trough (up to 1.4%Rr) and north of Maribor (up to 2.5%Rr) is extremely high (Sachsenhofer et al., 1998a, Fig. 3). The anomaly in the Ribnica–Selnica Trough is located north of a deeply eroded center of a Miocene volcano. Data from wells (Šomat 1, Benedikt 2/76, Pichla 1, Radkersburg 2, Figs. 3 and 4) show that the anomaly north of Maribor extends into the subsurface below immature middle and late Miocene sediments to the Radkersburg (Radgona) area, and is also connected with vitrinite reflectance anomalies in the vicinity of buried early/middle Miocene volcanoes in the Styrian Basin (Sachsenhofer, 1994). Vitrinite reflectance gradients in middle and late Miocene sediments are low (e.g. Radkersburg 2, Središče 1; Fig. 4).

Ljutomer Depression. Boreholes Gabrnik 1 (Fig. 3), Ljutomer 1, Dokležovje 1, Lipa 1, and Martin 1 (Fig. 4) are characterized by low vitrinite reflectance

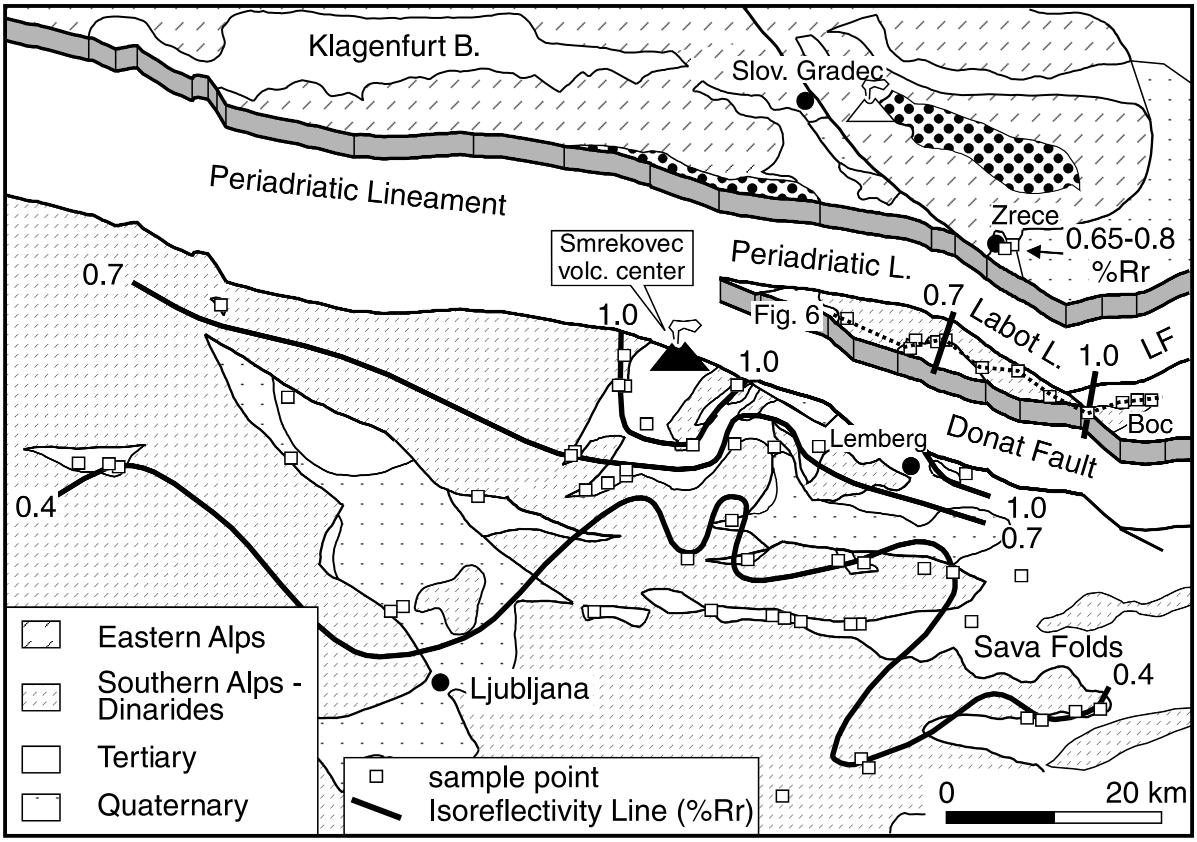

Fig. 5. Map showing vitrinite reflectance isolines for Eocene and Oligocene sediments north and south of the Donat Fault (see Fig. 1 for location of map). LF — Ljutomer Fault. Stippled line marks position of Fig. 6 cross-section.

gradients in middle and late Miocene sediments. In the Ljutomer 1 well 1.0%Rr is reached at 3500 m depth. No reflectance data are available from early Miocene sediments in the Ljutomer Depression.

4.2. Area between Periadriatic Lineament and Donat Fault zone

The stratigraphy of this region is not yet definitively resolved. West of the Labot Line an upper Eocene coal-bearing sequence occurs beneath early Miocene (Karpatian) deposits (Jelen et al., 1998a,b). Undated, but presumably Paleogene, coal-bearing sediments overlain by early Miocene sediments are also exposed east of the Labot Line in the Boč area (Fig. 3).

The location of Eocene samples together with isoreflectivity lines is shown in Fig. 5. Their vitrinite reflectance increases eastward from 0.5 to 1.5%Rr (Fig. 6). Vitrinite reflectance of early Miocene sediments is 0.5–0.6%Rr west of the Labot Line and increases dramatically east of the tectonic line. Note that vitrinite reflectance of Eocene and Miocene sediments is similar near Dobrna and Makole, but coalification of Eocene sediments is much higher compared to that of Miocene sediments between Črešnjice and the Labot Line (Fig. 6).

The area between the Periadriatic Lineament and the Donat Fault zone east of the Labot Line is dominated by two maxima, both located in early Miocene sediments (Fig. 3). They are aligned along the axis of the Boč Anticline. A western maximum borders the eastern end of Mt. Boč and it is separated from an eastern maximum by a N–S-trending corridor with relatively low vitrinite reflectance. Vitrinite reflectance of early Miocene (Karpatian) sediments increases from top to bottom from about 0.5 to

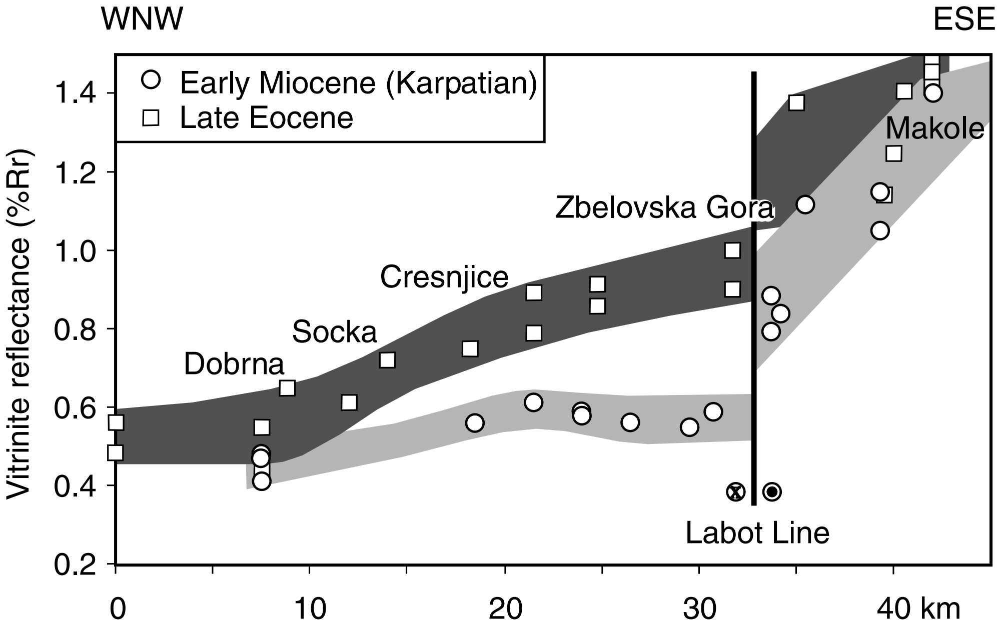

Fig. 6. Coalification of Eocene and overlying early Miocene (Karpatian) sediments along the crustal segment bordered by the Periadriatic Lineament and the Donat Fault. A gap in Eocene/early Miocene (Karpatian) coalification exists between Črešnjice and Zbelovska Gora. Vitrinite reflectance of early Miocene sediments increases dramatically east of the Labot Line (see Fig. 5 for location of cross-section).

1.6%Rr in the western anomaly and from 0.3 to 1.35%Rr in the eastern anomaly. Considering the relatively low thickness of the early Miocene sequence (500–800 m; Aničič and Juriša, 1984), very high reflectance gradients are obvious. Abrupt changes in coalification occur in the Boč area along WSW–ENE- and NW–SE-trending faults. In general, vitrinite reflectance of vertical-dipping middle/late Miocene (Sarmatian/Pannonian) coals along the northern margin of the Boč Anticline is low, but locally reaches 0.4%Rr.

Vitrinite reflectance curves of two wells (Murski Gozd 6, Petišovci 5) in the Ormož–Selnica Anticline are shown in Fig. 4. The observed vitrinite reflectance gradients in middle/late Miocene sediments are slightly higher than in the Ljutomer Depression. Reflectance gradients in early Miocene sediments are significantly higher.

4.3. Area south of (Periadriatic Lineament and) Donat Fault zone

Uppermost Eocene to earlimost Miocene (upper Egerian) sediments are widespread south of the Donat Fault zone. Eocene and Oligocene deposits, which are older than the main magmatic activity in the Smrekovec area, prevail west of the Labot Line, whereas younger sediments dominate in the eastern part.

West of Labot Line. Isoreflectivity lines for Eocene and Oligocene sediments are shown in Fig. 5. Vitrinite reflectance increases northward and reaches maximum values (up to 1.5%Rr) surrounding the Smrekovec volcanic center and along the Donat Fault. Vitrinite reflectance of early Miocene sediments, which are younger than the main magmatic activity, is generally low, but reaches 0.6%Rr in Egerian sediments close to the Donat Line near Lemberg (see Fig. 5 for position of Lemberg). In the entire region vitrinite reflectance of middle Miocene samples is about 0.3%Rr.

Plots of vitrinite reflectance versus depth were constructed for well Velenje P-12o/92, the Sava Folds (using surface data and information from well Td 1/84; Hamrla, 1989), and for the area around the Smrekovec volcanic center (Fig. 4). Data from the Lemberg area are included in the latter plot. No coalification break exists at the unconformity between

Oligo-/Miocene and middle Miocene (Badenian) sediments in the Sava Folds, but the reflectance gradient is much higher in pre-middle Miocene deposits than in younger sediments. In the Lemberg area a coalification break between earlimost Miocene (Egerian: 0.49–0.60%Rr) and middle Miocene sediments (Badenian: 0.29%Rr) is obvious.

Eastern portion. Vitrinite reflectance of Oligo-/Miocene (Egerian) sediments south of the Donat Fault zone ranges from 0.3 to 0.75%Rr (Fig. 3). Although the vitrinite reflectance is significantly lower than that of early Miocene (Karpatian) sediments north of it, some similarities in the reflectance patterns are observed. Areas with relatively high vitrinite reflectance are located opposite to the reflectance maxima north of the Donat Fault zone, and areas with low reflectance values (< 0.4%Rr) occur in the southern continuation of the above described N–S-trending zone, which separates two reflectance maxima east of Mt. Boč.

The Sava–Celje Fault separates Oligo-/Miocene (Egerian) sediments with up to 0.75%Rr to the north from coeval coal-bearing sequences with lower maturity (0.35–0.47%Rr) to the south. The latter are unconformably overlain by middle Miocene (Badenian) to Pliocene sediments. Although only one middle Miocene reflectance value (0.34%Rr) is available from this part of the study area, it is reasonable to assume that vitrinite reflectance of middle Miocene sediments south of the Donat Fault zone is generally < 0.4%Rr (see also western portion). Therefore, south of the Sava–Celje Fault, the 0.4% isoreflectivity line in Fig. 3 roughly follows the unconformity between Oligo-/Miocene and middle Miocene sediments. Note that in contrast to Mt. Boč, coalification along the margins of pre-Tertiary domains south of the Donat Fault zone (e.g. Ravna Gora) is low (< 0.5%Rr).

5. Thermochronology

The fission-track samples were collected from the Boč area (Fig. 3). Samples Sac-33/97, Slo-103/97 and Slo-115/97 are early Miocene (Karpatian) in age. Samples Slo-39/97 and Slo-93/97 are also from the base of the Neogene sequence, but are undated. The sediment derived from a slowly eroding, chemically strongly weathered surface; therefore the proportion of quartz and the resistant heavy minerals (Zircon + Turmaline + Rutile) is high, while the samples are very poor in apatite grains. Thus, age determination was possible only by using a limited number of crystals. For similar reasons confined track length measurement was achieved only on sample Sac-33/97.

The results are listed in Table 2. The vitrinite reflectance values of the Neogene sediments show that in the sampled zones of the basin, the post-depositional thermal overprint caused total annealing of the fission-tracks in apatite (Gleadow et al., 1983). In these siliciclastic sediment samples, all the apatite crystals had lost their inherited fission-track ages and the reset fission-track ages of the grains mark the cooling period after the thermal climax (all samples passed the chi-square test). The apparent fission-track ages scatter around 12 Ma indicating the cessation of the post-depositional thermal overprint 4–7 Ma after the sedimentation. The confined track length distribution of Sac-33/97 sample (Fig. 7) is composed of mainly unshortened tracks with some contribution of annealed ones. Fewer confined tracks were found in sample Slo-103/97. Although the two samples have similar track length, the age of Slo-103 is slightly younger, suggesting some slight areal variation in the cooling rate. Thermal modeling of the fission-track data was made by the method of Ketcham et al. (2000) using the annealing model of Laslett et al. (1987). The time/temperature history yielded by this procedure is not very meaningful. However, a period of a more rapid cooling during 15–12 Ma and a later slowly cooling interval can be distinguished (Fig. 7).

6. Numeric modeling of the thermal history

Fifteen wells have been selected for numerical modeling. An additional model was estimated for the Boč Anticline. Subsidence curves, reconstructed heat flow histories, and calibration data for seven wells are presented in Figs. 8 and 9. The regional distribution of reconstructed heat flows is shown in Fig. 10. This figure is based on all wells discussed in the present study and on published data from sites located in the Styrian Basin and the Radgona Depression (Sachsenhofer, 1994; Sachsenhofer et al., 1998b).

Table 2
Fission-track results from the Boč area

Sample number	Locality	Lithology	Rr[a] (%)	Crystals	Ps[b]	(Ns)[c]	Pi	(Ni)	Pd	(Nd)	$P(\chi^2)$[d] (%)	FT age[e] (Ma ± 1s)	Track length (n) (μm)
Sac-33/97	Goli Vrh	Sandstone	1.30	24	1.91	(294)	12.9	(1984)	5.12	(6232)	64	14.1±0.9	14.4±1.4 (62)
Slo-115/97	Gorenjci	Conglom.	1.06	25	0.92	(137)	6.47	(1040)	4.46	(4486)	62	11.0±1.0	N.D[f]
Sl0-103/97	Prihova	Conglom.	1.10	21	2.67	(263)	17.3	(1791)	4.46	(4486)	63	12.2±0.9	14.9±1.3 (31)
Slo-39/97	Stari Grad	Sandstone	1.54	25	1.14	(193)	8.58	(1509)	5.12	(6232)	80	12.2±1.0	15.2±1.3 (6)
Slo-39/97a	Stari Grad	Sandstone	1.54	25	1.02	(149)	8.99	(1334)	5.12	(6232)	37	10.7±1.0	N.D.
Slo-93/97	Stari Grad	Sandstone	> 1.5	22	0.69	(80)	6.28	(741)	5.12	(6232)	39	10.3±1.2	N.D.

[a] Rr = vitrinite reflectance.
[b] P = track densities as measured ($\times 10^5$tr/cm^2).
[c] N = number of tracks counted (shown in brackets)
[d] $P(\chi^2)$ = probability of obtaining χ^2 value for n (number of crystals − 1) degree of freedom.
[e] FT age = apatite fission-track ages calculated using dosimeter glass CN 5 with zeta = 373.3 ± 7.1.
[f] N.D. = not determined.

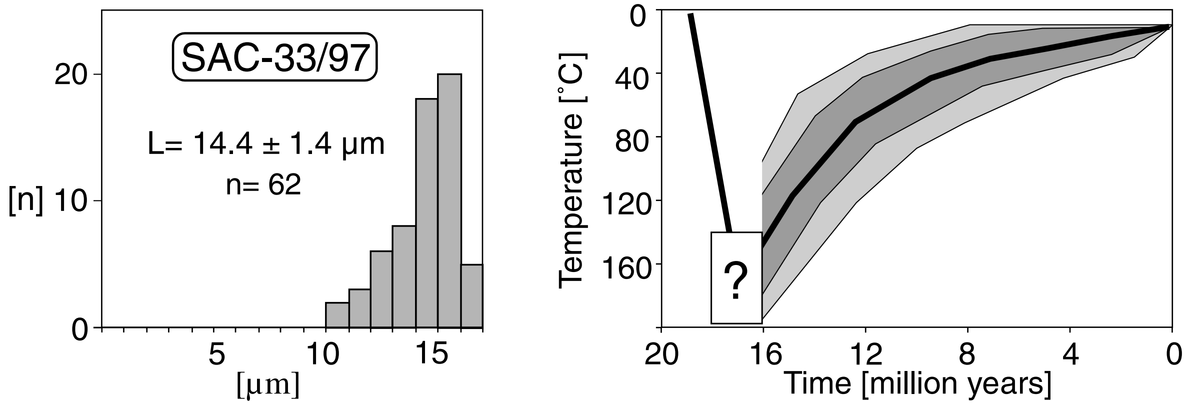

Fig. 7. Confined track length distribution of sample Sac-33/97 and inferred temperature history computed by the AFTSOLVE program (Ketcham et al., 2000). Bold line gives mean temperature history; the light gray belt contains all acceptable temperature histories, and the dark gray one gives the envelope of well-fitting cooling curves.

6.1. Maribor–Radgona area (Šomat 1, Benedikt 2/76)

The Šomat 1 well, located east of Maribor, is characterized by a very high vitrinite reflectance gradient (Fig. 3). A close fit between measured and calculated reflectance values is achieved with an early Miocene (Karpatian) heat flow of 375 mW/m^2 (Fig. 8). The post-early Miocene heat flow history is difficult to determine, because it has no effect on the calculated reflectance data. In the model of Fig. 8, we use the same middle Miocene heat flow as in the Pichla 1 well, which is situated 10 km northwest of Šomat (Sachsenhofer, 1994). Present-day heat flow is about 100 mW/m^2 (Ravnik, 1991).

Few reflectance data are available from the Benedikt 2/76 well (Fig. 3). Therefore, heat flow reconstructions are poorly constrained. Assuming that the observed thickness of early Miocene sediments is the original one, a heat flow of more than 400 mW/m^2 has to be assumed to account for the high vitrinite reflectance values. However, a reduction of the thickness of the early Miocene sequence due to erosion or faulting cannot be excluded and results in a lower heat flow estimate. In any case, early Miocene heat flow must have been extremely high. In Fig. 8 we adopt the same early Miocene heat flow as in the Šomat 1 well. Under this assumption, a good calibration is obtained with a reduction of the thickness of the early Miocene sediments of 450 m. Formation temperatures (Ravnik, 1991) indicate a present-day heat flow of 145 mW/m^2.

Similar high early Miocene heat flows were reconstructed for the Maribor area, the Radkersburg 2 well (Sachsenhofer et al., 1998b) and for wells in the southern Styrian Basin (Sachsenhofer, 1994; Fig. 10). Nevertheless, the exact heat flow numbers should not be overemphasized. This is because the used software simulates conductive heat transfer, whereas flow of hot fluids is not considered. Obviously, the latter mechanism is important in areas with magmatic activity.

The late Miocene heat flow can be determined in the deep eastern Radgona Depression. Here it was 60 (Radkersburg 2, Središče 1) to 70 mW/m^2 (Pecarovci 1, Dankovci 1; Fig. 10).

6.2. Ljutomer Depression (Ljutomer 1, Gabrnik 1)

In the Ljutomer 1 and Gabrnik 1 wells, a good fit between measured and calculated calibration data is achieved using a heat flow of 70 mW/m^2 since late Miocene times (Fig. 8). Similar heat flows (60–75 mW/m^2) are reconstructed for other wells in the Ljutomer Depression (Dokležovje 1, Lipa 1, Rakičan 1, Martin 1; Fig. 10). The early Miocene heat flow cannot be determined, because early Miocene sediments in the Ljutomer Depression are thin and were thermally overprinted during Miocene/Pliocene maximum burial.

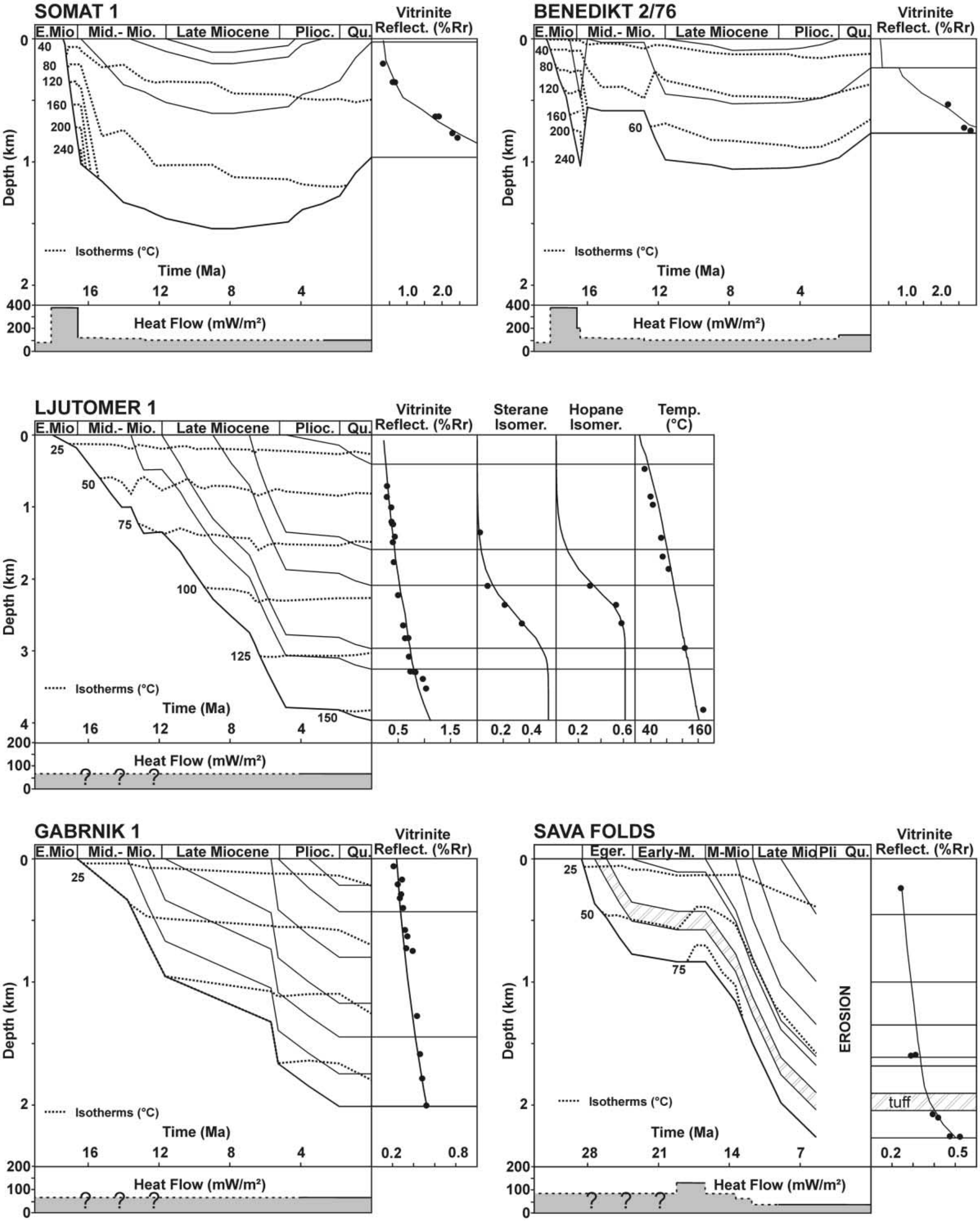

Fig. 8. Burial history, temperature history, and heat flow model of the Šomat 1, Benedikt 2/76, Ljutomer 1, and Gabrnik 1 wells, as well as for the Sava Folds. Heat flows are well defined only for the time of maximum temperatures and for the present. In the right part of the figures measured (dots) and calculated calibration data (solid line) are plotted vs. depth.

6.3. Area between Periadriatic Lineament and Donat Line (Murski Gozd 6, Petišovci 5)

Murski Gozd 6 and Petišovci 5 wells are located in the Ormož–Selnica Anticline. Seismic lines across the anticline (e.g. Durasek, 1988; Rumpler and Horváth, 1988; Pogácsás et al., 1994) prove young, post-Miocene uplift of the axial zone and allow estimates on thicknesses of eroded sediments. These are about 900 m for well Murski Gozd 6 and about 650 m for well Petišovci 5.

Two alternative heat flow models are shown for the Murski Gozd 6 well in Fig. 9:

- In the first model the heat flow was kept constant with time (90 mW/m^2). The calculated data are in accordance with recent temperatures and observed hopane isomerization. However, the fit between calculated and measured vitrinite reflectance and sterane isomerization values is poor (Fig. 9). Both, sterane isomerization and vitrinite reflectance of shallow samples (<3 km) is overestimated, whereas reflectance of deep early Miocene samples is underestimated.
- A reduction of heat flow to 85 mW/m^2 during late Miocene/Pliocene maximum burial results in a closer fit for sterane isomerization and for shallow vitrinite reflectance values. However, in this model middle Miocene (Badenian) heat flow has to be increased to 160 mW/m^2 in order to match vitrinite reflectance values of the deep samples. In addition, this second heat flow model correctly predicts reflectance values of Permo-Carboniferous sediments in the Ujfalu I well, which is situated 3.5 km east of Murski Gozd 6 (Laczó and Jámbor, 1988).

We favor the heat flow model with the middle Miocene heating event, which results in a better fit. However, at present the simple heat flow model cannot be ruled out. Note that adjusting the thickness of eroded sediments within a geologically meaningful range (500–1200 m) does not change the reconstructed heat flow histories significantly.

The Petišovci 5 well was modeled using a time-constant heat flow of 90 mW/m^2 (Fig. 9). Again, vitrinite reflectance values of shallow samples are slightly overestimated. However, in this well slightly underestimated sterane isomerization values suggest that 90 mW/m^2 may be a reasonable estimate for the late Miocene. High middle Miocene heat flow (e.g. 160 mW/m^2) has no effect on calculated calibration data, and therefore it cannot be excluded.

No well data are available from the Boč Anticline and only rough estimates on the thickness of sediments exist. The thickness of early Miocene sediments is 500–800 m according to Aničić and Juriš (1984). Winkler-Hermaden (1957) estimates that the entire Cenozoic sequence is 1500–2000 m thick. Because of these uncertainties, only first-order models were constructed, which only show the order of magnitude of early/middle Miocene heat flows. In order not to overestimate paleo-heat flows, we used maximum thickness values. The models show that extremely elevated early/middle Miocene heat flows ($\sim$200 mW/m^2) have to be assumed to fit the observed high coalification gradients and to take into account that early Miocene sediments cooled below 120°C by the end of the middle Miocene (11.8 ± 1.4 Ma).

6.4. Sava Folds (Td 1/84)

The Miocene/Pliocene subsidence history of the Sava Folds has been constructed using the stratigraphy of the Td 1/84 well (Hamrla, 1989) and adopting surface information (Petrica et al., 1995). A good calibration is achieved using elevated early Miocene heat flows (120–130 mW/m^2). It is impossible to determine the timing more precisely. It is likely that elevated heat flows occurred during late early Miocene time, when heat flow was extremely high in the Maribor and Boč areas, but an earlier heating cannot be excluded. In Fig. 8 a heat flow scenario with elevated late early Miocene heat flow is presented. Late Miocene heat flow is approximately 40 mW/m^2.

7. Discussion

7.1. General

Sometimes it is difficult to distinguish the effects of different heat flow and burial/unroofing histories on vitrinite reflectance. A final decision is possible if reflectance data are available over a profile with known thickness and stratigraphy. This is the case in studied wells and in the studied surface areas east of

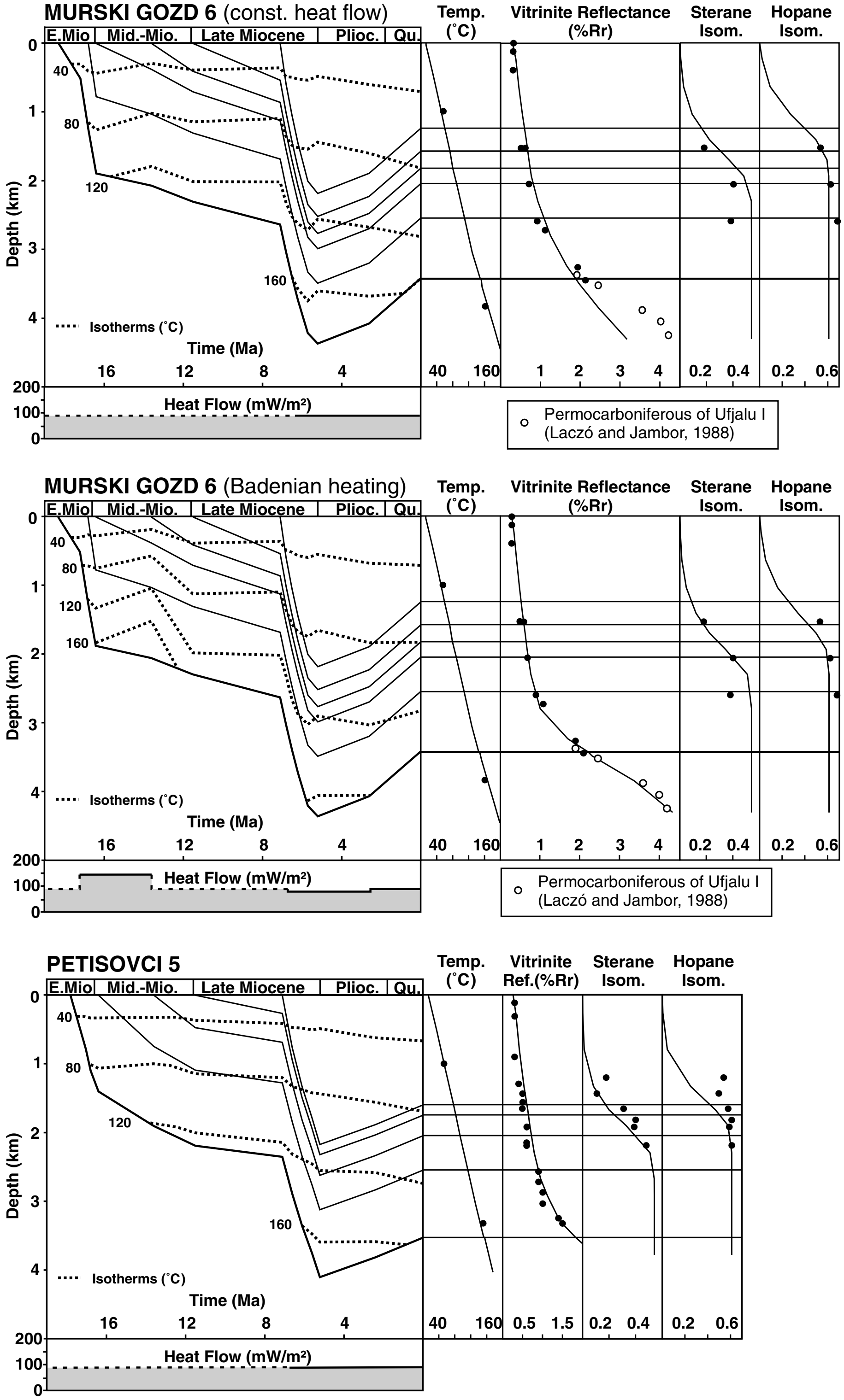
MURSKI GOZD 6 (const. heat flow)
E.Mio
Mid.-Mio.
Late Miocene
Plioc.
Qu.
Depth (km)
Isotherms (˚C)
Time (Ma)
Heat Flow (mW/m²)
Temp. (˚C)
Vitrinite Reflectance (%Rr)
Sterane Isom.
Hopane Isom.
Permocarboniferous of Ufjalu I (Laczó and Jambor, 1988)
MURSKI GOZD 6 (Badenian heating)
E.Mio
Mid.-Mio.
Late Miocene
Plioc.
Qu.
Depth (km)
Isotherms (˚C)
Time (Ma)
Heat Flow (mW/m²)
Temp. (˚C)
Vitrinite Reflectance (%Rr)
Sterane Isom.
Hopane Isom.
Permocarboniferous of Ufjalu I (Laczó and Jambor, 1988)
PETISOVCI 5
E.Mio
Mid.-Mio.
Late Miocene
Plioc.
Qu.
Depth (km)
Isotherms (˚C)
Time (Ma)
Heat Flow (mW/m²)
Temp. (˚C)
Vitrinite Ref.(%Rr)
Sterane Isom.
Hopane Isom.

the Labot Line, where fission track ages provide additional constraints on the reconstructed thermal histories. The situation is less favourable in the area west of the Labot Line. However, vitrinite reflectance maps and an observed break in vitrinite reflectance between Paleogene and early Miocene sediments allows straightforward interpretations. The quality of paleo-heat flow estimates depends on many factors, like availability of different calibration data and the knowledge of burial histories and of the physical properties of preserved and eroded sediments. We changed paleo-heat flow estimates, physical properties of sediments (e.g. thermal conductivities) and adjusted the eroded thickness of sediments in order to estimate the uncertainty of our results. It is concluded that the uncertainty is about 10% of the paleo-heat flow estimate for most wells. It has already been stated that in areas with magmatic activity the uncertainty of paleo-heat flow estimates is higher. Partly, this is because of the use of 1-D models in areas with high lateral heat flow variations. Therefore, the exact numbers of the reconstructed heat flows should not be overemphasized.

7.2. Oligocene thermal evolution

Breaks in coalification patterns between Paleogene and early Miocene (Karpatian) sediments indicate that Paleogene sediments in the Smrekovec area, the crustal slice bordered by the Periadriatic Lineament, Donat Fault and Labot Line, and the Zreče area matured before deposition of early Miocene sediments. Thus, vitrinite reflectance in these areas provides information on Oligocene thermal conditions.

There is a clear spatial relationship between the vitrinite reflectance anomaly in the Smrekovec area and the center of Oligocene volcanism (Fig. 5). Thus, we consider the magmatic activity as the main heat source during Oligocene time.

The high pre-Miocene (pre-Karpatian) coalification between Črešnjice and the Labot Line in the crustal slice bordered by the Periadriatic Lineament and Donat Fault (Fig. 6) was caused by thermal perturbations near the Smrekovec volcano. This interpretation and the eastward increase in coalification imply that the crustal slice was originally situated west of Smrekovec, and that dextral movements along the Donat Fault transported it to its present-day position. Right-lateral offset is estimated to be at least 50 km. Tectonic investigations by Fodor et al. (1998) confirm early Miocene (pre-Karpatian) dextral movements along the Donat Fault.

Relatively high pre-middle Miocene coalification of Oligo-/Miocene sediments along the Donat Fault zone east of Smrekovec and the reconstructed heat flow history in the Sava Folds (Td 1/84 well) indicate that at least locally heat flow increased during early Miocene times. At present, it cannot be decided if this is because heat flow remained high after the Oligocene magmatic event until early Miocene times, or heating was caused by a separate early Miocene heating event.

At Zreče, the missing correlation between the age of upper Cretaceous to Eocene coals and their vitrinite reflectance indicates that Cretaceous and Paleogene sediments matured together after a late Eocene/early Oligocene tectonic event. This maturation occurred before the early Miocene (Karpatian), probably as a result of the emplacement of the Oligocene Pohorje pluton (Hamrla, 1988).

7.3. Early/middle Miocene thermal evolution

Numerical heat flow reconstructions suggest that early/middle Miocene (Karpatian/ Badenian) heat flow at the eastern end of the Alps was on the order of >200 mW/m^2 (Fig. 10). Apatite fission-track ages show that the thermal overprint had terminated by middle Miocene time (14.4 ± 2.3 Ma, Sachsenhofer et al., 1998a,b) in the Maribor area. Early Miocene sediments in the Boč area cooled below 120°C only during middle/late Miocene (11.8 ± 1.4 Ma) time.

High heat flow in the Styrian Basin is a result of Miocene magmatic activity. The same is true for the

Fig. 9. Burial history, temperature history, and heat flow models of the Murski Gozd 6 and Petišovci 5 wells. In the right part of the figures measured (dots) and calculated calibration data (solid line) are plotted vs. depth. Two different heat flow models are shown for the Murski Gozd 6 well. Note the better fit between measured and calculated vitrinite reflectance and sterane isomerization values in the model including a Badenian heating event. Vitrinite reflectance data of Permocarboniferous sediments in the Ujfalu I well (Laczó and Jambor, 1988) are also shown.

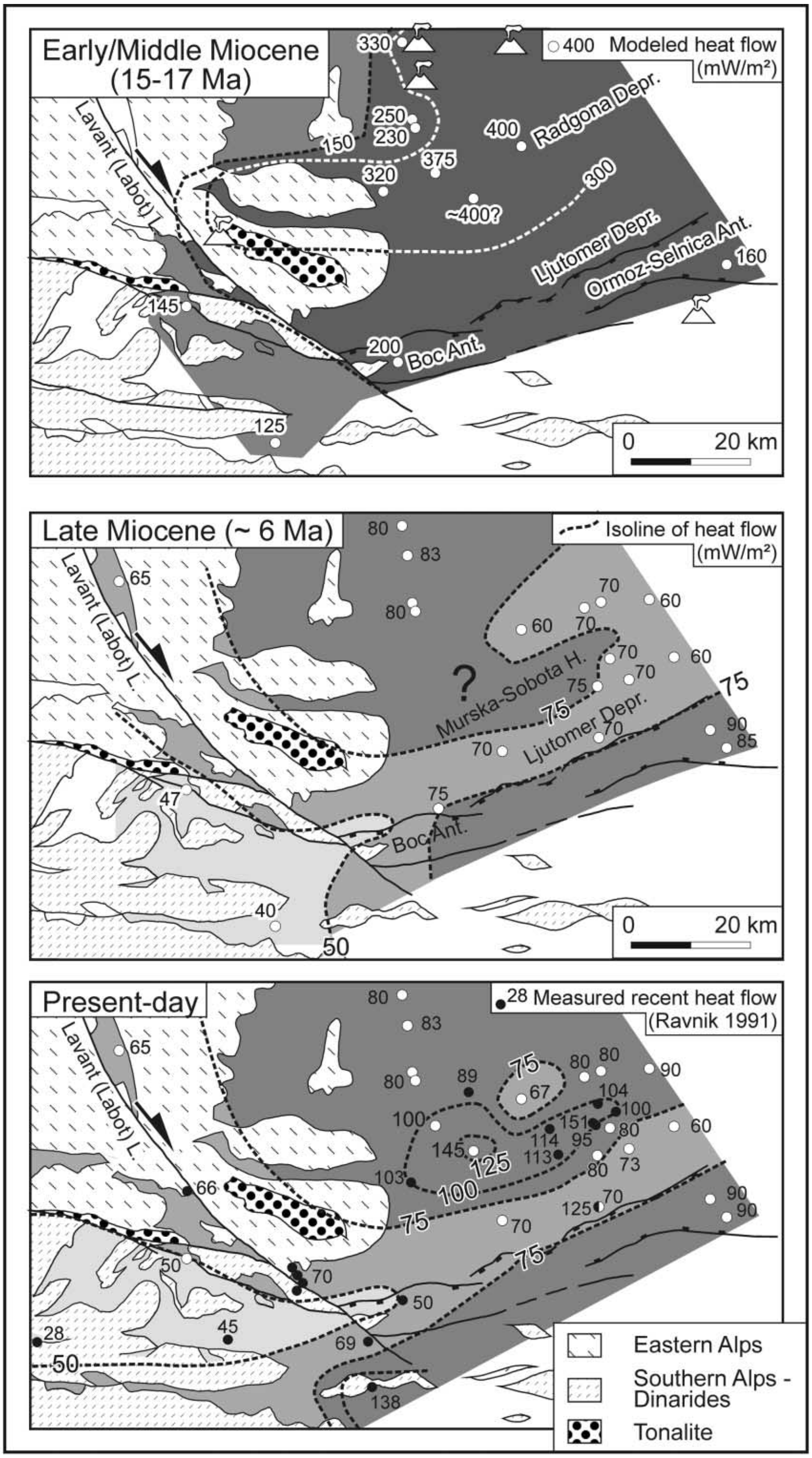

Fig. 10. Regional distribution of reconstructed heat flows for early/middle Miocene (Karpatian/Badenian), late Miocene/Pliocene (maximum burial), and Recent time. Measured present-day heat flow data from additional wells are included (Ravnik, 1991). With the exception of the Ljutomer 1 well, there is a good agreement between recent heat flows derived from basin modeling and geothermal investigations (e.g. Ravnik, 1991). Note that isolines are hand-contoured and in some areas speculative.

Ribnica–Selnica Trough, which was heated by Miocene dacitic magmatism in the western Pohorje area. It is possible that this magmatic event also resulted in relatively high vitrinite reflectance SE of Slovenj Gradec (up to 0.78%Rr). The heat source for the vitrinite reflectance anomaly north of Maribor (see Fig. 3) and its eastern subsurface continuation (Šomat–Benedikt–Radkersburg) is less obvious, because no magmatic rocks are known from this area. Sachsenhofer et al. (1998a,b) discussed two possible explanations:

- A large shallow early/middle Miocene pluton beneath the vitrinite reflectance anomaly.
- Advective heat transport due to subvertical displacement of hot rock bodies (e.g. Dunkl et al., 1998). Rapid early Miocene uplift of metamorphic rocks of the Kozjak/Pohorje region is shown by fission-track ages of detrital apatite grains in early Miocene sediments (Sachsenhofer et al., 1998a,b).

We prefer the first explanation, although the postulated magma chamber, which connects the Miocene volcanic centers in the Pohorje area and in the Styrian Basin, has not been identified by geophysical methods.

It is even more difficult to find the heat source for the Boč area. This is because the area is situated about 35 km from the next magmatic center (western Pohorje) and no nearby metamorphic core complex is known. Thus, we speculate: e.g. that the early Miocene position of the Boč area was closer to the Pohorje Mountain, and that varying displacements along strike of the Labot Line increased the distance.

The northern margin of the area with extremely elevated early/middle Miocene heat flow is located in the northern Styrian Basin and is controlled by the position of volcanoes and the coeval rapid uplift of the Rechnitz Window (Sachsenhofer, 1994; Dunkl et al., 1998). The southwestern margin of the anomaly was probably located close to the position of the Labot Line. This is suggested by the rapid westward decrease in vitrinite reflectance of early Miocene sediments, both in the Boč area west of Makole (Fig. 6) and in the Slovenj Gradec area, and agrees with early Miocene heat flows, which were only on the order of 120–150 mW/m^2 in the Sava Folds (Td 1/84 well) and the Velenje area (P-12o/92) west of the Labot Line. Even lower heat flows are possible when maximum temperatures occurred already during the Oligo-/Miocene, whereas higher heat flows can be excluded. The southern and eastern border of the region with high heat flow cannot be defined. This is because early Miocene sediments in the Ljutomer Depression and east of Radgona are either missing, or were thermally overprinted during deep late Miocene burial.

Most probably, the Ormož-Selnica Anticline was affected by a middle Miocene (Badenian) thermal event. Extensive contemporaneous magmatism southwest of Murski Gozd (Pamic and Pécskay, 1996) represents a possible heat source. Laczó and Jámbor (1988) postulated a magmatic heating event in this region based on high vitrinite reflectance gradients in Permo-Carboniferous sediments in the Ujfalu I well. Perhaps these late Paleozoic sediments matured only during middle Miocene times. However, because the heat flow reconstruction for the Murski Gozd 6 well is equivocal, an earlier magmatic event cannot be ruled out.

7.4. Post-middle Miocene thermal evolution

Wells in northeastern Slovenia with middle and late Miocene sediments provide information on the post-middle Miocene thermal history. The regional distribution of late Miocene/Pliocene heat flow and a recent heat flow map are shown in Fig. 10.

The Late Miocene/Pliocene heat flow pattern is characterized by very low heat flow in the Sava Folds and the Velenje area (<50 mW/m^2) and by moderate heat flow in the Ljutomer and Radgona Depressions (60–75 mW/m^2). Higher heat flow occurred in the southern Styrian Basin and along the Ormož–Selnica Anticline (80–90 mW/m^2). Possible explanations for the higher heat flow in the Ormož–Selnica Anticline include thermal effects due to young, rapid erosion, hydrodynamic systems, or an inherited higher heat flow from a former extensional stage of basin formation. No data are available from the Murska–Sobota High. However, because it is frequently observed that heat flow is higher along basement highs than in deep basins, we assume that heat flow was above 80 mW/m^2 (Fig. 10). Note that despite of thinned crust beneath the western Pannonian Basin heat flow was relatively low in the deep troughs. Perhaps, this is due to the thermal blanketing effect of rapidly deposited sediments (e.g. Lenkey, 1999).

In general, the present-day heat flow pattern is similar to the late Miocene one (Fig. 10). However, heat flow increased in the Radgona Depression and a present-day heat flow anomaly occurs in the Šomat–Benedikt area (up to 145 mW/m^2; Ravnik et al., 1995). Probably, the latter is caused by hydrodynamic systems.

7.5. Vitrinite reflectance and late-stage uplift of the Boč Anticline

The alignment of vitrinite reflectance maxima along the fold axis of the Boč Anticline is clearly a result of late stage basin inversion. Thus, virinite reflectance patterns provide information on this late-stage tectonic event.

The thickness of the Tertiary sediments is on the order of 1.5–2 km. An uplift on the order of 2.5–3 km is estimated, when the elevation of the peak of Mt. Boč (979 m) is taken into account. Differences in vitrinite reflectance along the anticline indicate an undulation of its WSW–ENE-trending fold axis. Jumps in vitrinite reflectance along faults north and east of Mt. Boč are evidence for vertical and lateral displacements on the order of several hundred meters. Vertical displacements with the same order of magnitude occurred along the Donat Fault zone forming the southern margin of the Boč Anticline. Vitrinite reflectance patterns (Fig. 3) clearly show the relative uplift of the northern domain along this fault and along the Sava–Celje Fault.

In spite of the postulated movements along the Donat Fault, reflectance maxima and minima north and south of it are located roughly opposite each other. For example, the low-coalification corridor east of Mt. Boč continues into a vitrinite reflectance minimum south of the Donat Fault zone (Fig. 3). Therefore, vitrinite reflectance patterns suggest that no major late-stage lateral displacements occurred along the Donat Fault zone. However, post-Miocene dextral movements were postulated by Fodor et al. (1998) based on paleomagnetic results for the Ormož–Selnica Anticline and microtectonic measurements.

8. Conclusions

Our investigations revealed the following thermal history in the transition zone between Eastern Alps, Southern Alps–Dinarides, and the Pannonian Basin:

8.1. Oligocene thermal evolution

Pre-early Miocene (pre-Karpatian) vitrinite reflectance patterns allow statements on the thermal conditions prior to the continental escape of the Eastern Alps. Oligocene (Smrekovec) volcanism was the main heat source for Paleogene sediments south of the Periadriatic Lineament, whereas relatively high vitrinite reflectance of upper Cretaceous to Paleogene coal-bearing sequences south of the Pohorje is probably a result of the emplacement of the Pohorje tonalite. Vitrinite reflectance patterns suggest dextral displacements on the order of 50 km along the Donat Fault zone.

8.2. Early/middle Miocene thermal evolution

Early/middle Miocene (Karpatian/Badenian) heat flows of more than 200 mW/m^2 were reconstructed for the Ribnica–Selnica Trough, the Maribor–Radgona area, and the Styrian Basin. Because fluid flow was not considered in our models, the exact heat flow values should not be overemphasized. At least partly, the extremely elevated heat flows are a consequence of magmatic activity in the Styrian Basin and the western Pohorje. No magmatic rocks are known from the Maribor–Radgona area. A large shallow early/middle Miocene pluton (magma chamber) could explain the observed Miocene heat flow. Perhaps, rapid uplift of hot basement rocks in the Pohorje/Kozjak region, which is documented by apatite fission-track dating, also increased surface heat flow.

Extremely high early/middle Miocene heat flow also occurred along the Boč and Ormož–Selnica Anticlines. Badenian volcanism south of the latter anticline represents a potential heat source. The heat source for the Boč Anticline is unknown, because neither volcanic rocks nor metamorphic core complexes are known from this area.

Obviously, early/middle Miocene heat flow over large areas within the western Pannonian realm was extremely high. Therefore, its influence on crustal rheology and basin forming processes during the early/middle Miocene syn-rift phase has to be taken into account (e.g. Tari and Horváth, 1995; Sachsenhofer et al., 1997).

8.3. Post-middle Miocene thermal evolution

The late Miocene post-rift phase of the study area was characterized by slightly elevated heat flows, caused by thinned crust beneath the Pannonian realm. Moderate Neogene heat flows occurred in the Radgona and Ljutomer Depressions (60–75 mW/m^2) and along the Ormož–Selnica Anticline (85–90 mW/m^2). A present-day heat flow anomaly occurs in the Šomat–Benedikt area.

8.4. Late-stage basin inversion in the Boč area

High vitrinite reflectance of surface samples along the fold axis of the Boč Anticline is a result of an early/middle Miocene thermal event and late-stage basin inversion. Post-middle Miocene uplift of the pre-Tertiary Mt. Boč, forming the most exhumed part of the Boč Anticline, was on the order of 2500–3000 m. The Donat Fault zone is the southern border of the Boč Anticline. Vitrinite reflectance patterns indicate late-stage uplift of the northern block along this fault and along the Sava–Celje Fault.

Acknowledgements

The authors express their gratitude to the Austrian Science Foundation (FWF) for funding this study in the framework of project P10738-TEC. B.J. was supported by The Ministry of Science and Technology of the Republic of Slovenia, research grant No. JI-7018-0215. Samples and a wealth of geological information were kindly provided by Nafta Lendava and Geoplin Ljubljana. We are especially grateful to staff members of the Institute for Petroleum and Organic Geochemistry (ICG-4), KFA Jülich, Germany for determining biomarker ratios. The German Science Foundation supported the fission-track part of this study in the frame of the Collaborative Research Centre 275. The paper benefited greatly from discussions with C. Büker (Bern), L. Lenkey, L. Fodor and E. Márton (Budapest). Critical reviews of an early version of the paper by R.A. Ketcham and L.H. Royden are gratefully acknowledged.

References

Aničič, B., Juriša, M., 1984. Osnova geološka karta SFRJ, Rogatec: Zvezni geološki zavod, Beograd, scale 1:100,000, 1 sheet.

Barić, G., Britvić, V., Dragaš, M., 1996. Source rocks and hydrocarbon accumulations in the Mura Depression, Republic of Croatia. Nafta 47, 25–34.

Brezigar, A., Ogorelec, B., Rijavec, L., Mioč, P., 1987. Geološka zgradba predpliocenske podlage Velenjske udorine in okolice. Geologija 30, 31–65.

Buck, 1991. Modes of continental lithospheric extension. J. Geophys. Res. 96, 163–168.

Csontos, L., Nagymarosy, A., Horváth, F., Kovác, M., 1992. Model for the Tertiary evolution of the Intra-Carpathian area. Tectonophysics 208, 21–241.

Dövényi, P., Horváth, F., 1988. A review of temperature, thermal conductivity, and heat flow data for the Pannonian Basin. In: Royden, L.H., Horváth, F. (Eds.), The Pannonian basin. A study in basin evolution. Am. Assoc. Pet. Geol. Mem. 45, 195–233.

Dunkl, I., Grasemann, B., Frisch, W., 1998. Thermal effects of exhumation on hanging wall syn-rift sediments: an example from the Rechnitz Window Eastern Alps. Tectonophysics 297, 31–50.

Durasek, St., 1988. Rezultati suvremenih geofickih istrazivanja u SR Sloveniji (1985–1987). Nafta 39, 311–326.

Durasek, St., 1991. Pregledna karta podlage terciarja Murske depresije, Nafta Lendava, scale 1:100,000, 1 sheet, internal report.

Ebner, F., Sachsenhofer, R.F., 1995. Paleogeography, subsidence and thermal history of the Neogene Styrian Basin (Pannonian basin system, Austria). Tectonophysics 242, 133–150.

Exner, C., 1976. Die geologische Position der Magmatite des periadriatischen Lineamentes. Verh. Geol. Bundesanst. 1976, 3–64.

Faninger, E., 1970. Pohorski tonalit in njegovi diferenciati. Geologija 13, 35–104.

Fodor, L., Jelen, B., Márton, E., Skaberne, D., Car, J., Vrabec, M., 1998. Miocene–Pliocene tectonic evolution of the Slovenian Periadriatic fault: Implications for Alpine–Carpathian extrusion models. Tectonics 17, 690–709.

Frisch, W., Kuhlemann, J., Dunkl, I., Brügel, A., 1998. Palinspastic reconstruction and topographic evolution of the Eastern Alps during Late Tertiary tectonic extrusion. Tectonophysics 297, 1–15.

Frisch, W., Dunkl, I., Kuhlemann, J., 2000. Post-collisional orogen-parallel large-scale extension in the Eastern Alps. Tectonophysics 327, 239–265.

Gleadow, A.J.W., Duddy, I.R., Lovering, J.F., 1983. Fission track analysis: a new tool for the evaluation of thermal histories and hydrocarbon potential. Australian Petroleum Exploration Assoc. J. 23, 93–102.

Hamrla, M., 1985/1986. Light reflectance of some Slovenian coals. Geologija 28/29, 293–317.

Hamrla, M., 1988. Contribution to the geology of coal deposits in the Zreče area and reflectance-based ranking of its coal. Geologija 30, 343–390.

Hamrla, M., 1989. Progresije in gradienti odsevnosti vitrinita v nekaterih vrtinah severovzhodne slovenije. Rudarsko-Metalurski Zbornik 36, 371–381.

Harangi, Sz., Wilson, M., Tonarini, S., 1995. Petrogenesis of Neogene potassic volcanic rocks in the Pannonian Basin. In: Downes, H., Vaselli, O. (Eds.), Neogene and Related Magmatism in the Carpatho-Pannonian Region. Acta Vulcanologica 7, pp. 125–134.

Hasenhüttl, C., Kraljic, M., Sachsenhofer, R.F., Jelen, B., Rieger, R., 2001. Source rocks and hydrocarbon generation in Slovenia (Mura Depression, Pannonian Basin). Mar. Pet. Geol. 18, 115–132.

Horváth, F., 1993. Towards a mechanical model for the formation of the Pannonian basin. Tectonophysics 226, 333–357.

Horváth, F., 1995. Hydrocarbon plays and perspectivity in the Pannonian Basin. In: Horváth, F., Tari, G., Bokor, C. (Eds.), Extensional collapse of the Alpine orogene and hydrocarbon prospects in the basement and basin fill of the western Pannonian Basin. AAPG International Conference Exhibition, Nice, France, Guidebook to fieldtrip No. 6, Hungary, pp. 157–169.

Jelen, B., 1985/86. Poizkus iskanla organskih parametrov terciarnih sedimentnih kamenin v vzhodni Sloveniji. Geologija 28/29, 183–197.

Jelen, B., 1992. Model of positional relationships for Upper Paleogene and Miocene strata in Slovenia. IUGS-SOG Meeting Ancona, Abstracts and field trips, pp. 71–72.

Jelen, B., Báldi, M., Rifelj, H., 1998a. Recent improvements in Slovenian upper Paleogene and lower Miocene time-rock stratigraphy. Carpathian–Balkan Geol. Assoc. XVI Congress, Vienna, Abstracts, p. 248.

Jelen, B., Márton, E., Fodor, L., Báldi, M., Čar, J., Rifelj, H., Skaberne, D., Vrabec, M., 1998b. Paleomagnetic, tectonic and stratigraphic correlation of Tertiary formations in Slovenia and Hungary along the Periadriatic and mid-Hungarian tectonic zone (preliminary communication). Geologija 40, 325–331.

Kázmér, M., 1984. Continental escape of the Bakony–Drauzug unit in the Paleogene. Áltlalános Földtani Szemle 20, 55–102.

Kázmér, M., Kovács, S., 1985. Permian-Paleogene paleogeography along the eastern part of the Insubric-Periadriatic Lineament system: Evidence for continental escape of the Bakony–Drauzug unit. Acta Geol. Hung. 28, 71–84.

Kázmér, M., Fodor, L., Józsa, S., Jelen, B., Herlec, U., Kuhlemann, J., 1996. Late Miocene paleogeography of Slovenia and the Southern Alps: A palinspastic approach. In: Amann, G. (Ed.). Tektonik-Strukturgologie-Kristallingeologie. Facultas-Universitätsverlag, Salzburg, pp. 212–214.

Ketcham, R.A., Donelick, R.A., Donelick, M.B., 2000. AFTsolve: program for multi-kinetic modeling of apatite fission-track data. Geol. Material Res. 2, 1–32.

Laczó, I., Jámbor, Á., 1988. Secondary heating of vitrinite: Some geological implications. In: Royden, L.H., Horváth, F., (Eds), The Pannonian Basin. A Study in Basin Evolution. Am. Assoc. Pet. Geol. Mem. 45, 311–318.

Lankreijer, A.C., 1998. Rheology and basement control on extensional basin evolution in Central and Eastern Europe: Variscan and Alpine–Carpathian–Pannonian tectonics. PhD Thesis, Amsterdam, Vrije Universiteit, 157 pp.

Laslett, G.M., Green, P.F., Duddy, I.R., Gleadow, A.J.W., 1987. Thermal annealing of fission tracks in apatite 2. A quantitative analysis. Chem. Geol. 65, 1–13.

Laubscher, H.P., 1983. The late Alpine (Periadriatic) intrusions and the Insubric Line. Mem. Soc. Geol. Italia 26, 21–30.

Lenkey, L., 1999. Geothermics of the Pannonian Basin and its bearing on the tectonics of basin evolution. PhD Thesis, Amsterdam, Vrije Universiteit, 215 pp.

Mackenzie, A.S., 1984. Applications of biological markers in petroleum geochemistry. In: Welte, D.H. (Ed.), Advances in Petroleum Geochemistry, 1. Academic Press, London, pp. 115–214.

Mackenzie, A.S., McKenzie, D.P., 1983. Aromatization and isomerization of hydrocarbons in sedimentary basins formed by extension. Geol. Magazine 120, 417–470.

Odin, G.S., 1994. Premiers âges géochronologiques di niveaux volcanoclastiques olgicènes de la Région de Zasavje, Slovénie. G. Geol. Ser. 3 56, 199–212.

Pamic, J., Pécskay, Z., 1996. Geological and K-Ar ages of Tertiary volcanic formations from the southern part of the Pannonian Basin in Croatia — based on surface and subsurface data. Nafta 47, 195–202.

Petrica, R., Rijavec, L., Dozet, St., 1995. Stratigraphy of the Upper Oligocene and Miocene beds in the Trobni Dol area (Kozjansko) . Rudarsko-Metalurski zbornik 42, 127–141.

Pleničar, M., Hinterlechner-Ravnik., A., Faninger, E., 1990. Some tectonic elements and tectonic events on the SW margin of the Pannonian basin. In: International Symposium of Geodynamic evolution of the Pannonian basin, Academic Conferences, Beograd, Serbian Academy of Sciences and Arts 62, pp. 161–170.

Pogácsás, G., Mattick, R.E., Tari, G., Várnai, P., 1994. Structural control on hdrocarbon accumulation in the Pannonian Basin Hungary. In: Teleki, P.G. (Ed.), Basin Analysis in Petroleum Exploration. Kluwer Academic Publishers, Dordrecht, pp. 221–235.

Poljak, M., 1984. Neotectonic evolution in the Pannonian basin based on satellite images. Advances in Space Research 11, 139–146.

Premru, U., 1976. Neotektonica vzhodne Slovenije. Geologija 19, 211–249.

Premru, U., 1981. Tectonic evolution of Slovenia during the time interval from the upper Cretaceous to the Tertiary period (in Slovene with English summary): Symposium on problems of Danian in Jugoslavia, Ljubljana, Proceedings, pp. 147–154

Ratschbacher, L., Frisch, W., Linzer, H-G., Merle, O., 1991. Lateral extrusion in the Eastern Alps 2: Structural analysis. Tectonics 10, 257–271.

Ravnik, D., 1991. Geothermal investigations in Slovenia. Geologija 34, 265–303.

Ravnik, D., Rajver, D., Poljak, M., Živčič, M., 1995. Overview of the geothermal field of Slovenia in the area between the Alps, the Dinarides and the Pannonian basin. Tectonophysics 250, 135–149.

Rijavec, L., 1976. Biostratigrafija miocena v Slovenskih goricah. Geologija 19, 53–82.

Rögl, F., 1996. Stratigraphic correlation of the Paratethys Oligocene and Miocene. Mitt. Ges. Geol. Bergbaustud. Österreich 41, 65–73.

Royden, L.H., Horváth, F. (Eds), 1998. The Pannonian basin. A Study in Basin Evolution. Am. Assoc. Pet. Geol. Mem. 45, 394 pp.

Rumpler, J., Horváth, F., 1988. Some representative seismic reflection lines from the Pannonian Basin and their structural interpretation. In: Royden, L.H., Horváth, F. (Eds.), The Pannonian basin. A study in basin evolution. AAPG Mem. 45, 153–169.

Sachsenhofer, R.F., 1992. Coalification and thermal histories of Tertiary basins in relation to late Alpidic evolution of the Eastern Alps. Geol. Rundschau 81, 291–308.

Sachsenhofer, R.F., 1994. Petroleum generation and migration in the Styrian Basin (Pannonian Basin system Austria): An integrated geochemical and numeric modelling study. Mar. Pet. Geol. 11, 684–701.

Sachsenhofer, R.F., Lankreijer, A., Cloetingh, S., Ebner, F., 1997. Subsidence analysis and quantitative basin modelling in the Styrian Basin (Pannonian Basin system, Austria). Tectonophysics 272, 175–196.

Sachsenhofer, R.F., Dunkl, I., Hasenhüttl, Ch., Jelen, B., 1998a. Miocene thermal history of the southwestern margin of the Styrian Basin: vitrinite reflectance and fission track data from the Pohorje/Kozjak area (Slovenia). Tectonophysics 297, 17–29.

Sachsenhofer, R.F., Rantitsch, G., Hasenhüttl, C., Russegger, B., Jelen, B., 1998b. Smectite to illite diagenesis in early Miocene sediments from the hyperthermal western Pannonian Basin. Clay Minerals 33, 523–537.

Sweeney, J.J., Burnham, A.K., 1990. Evaluation of a simple model of vitrinite reflectance based on chemical kinetics. Am. Assoc. Pet. Geol. Bull. 74, 1559–1570.

Tari, G., Báldi, T., Báldi-Beke, M., 1993. Paleogene retroarc flexural basin beneath the Neogene Pannonian basin: a geodynamic model. Tectonophysics 226, 433–455.

Tari, G., Horváth, F., 1995. Middle Miocene extensional collapse in the Alpine–Pannonian transition zone. In: Horváth, F., Tari, G., Bokor, C. (Eds.), Extensional collapse of the Alpine orogene and hydrocarbon prospects in the basement and basin fill of the western Pannonian Basin. AAPG International Conference and Exhibition, Nice, France, Guidebook to fieldtrip No. 6, Hungary, pp. 75–105.

Tari, G., Horváth, F., Weir, G., 1995. Palinspastic reconstruction of the Alpine/Carpathian/Pannonian system. In: Horváth, F., Tari, G., Bokor, C. (Eds.), Extensional collapse of the Alpine orogene and hydrocarbon prospects in the basement and basin fill of the western Pannonian Basin. AAPG International Conference and Exhibition, Nice, France, Guidebook to fieldtrip No. 6, Hungary, pp. 119–132.

Tari, G., Dövényi, P., Dunkl, I., Horváth, F., Lenkey, L., Stefanescu, M., Szafián, P., Tóth, T., 1999. Lithospheric structure of the Pannonian basin derived from seismic, gravity and geothermal data. In: Durand, B., Jolivet, L., Horváth, F., Séranne, M. (Eds.), The Mediterranean Basins: Tertiary Extension within the Alpine Orogene. Geol. Soc. London Spec. Publ. 156, pp. 215–250.

Taylor, G.H., Teichmüller, M., Davis, A., Diessel, C.F.K., Littke, R., Robert, P., 1998. Organic Petrology. Gebrüder Borntraeger, Berlin, 704 pp.

von Blankenburg, F., Davies, J.H., 1995. Slab breakoff: A model for syncollisional magmatism and tectonics in the Alps. Tectonics 14, 120–131.

Winkler-Hermaden, A., 1957. Geologisches Kräftespiel und Landformung. Springer, Vienna, 822 pp.

Wygrala, B.P., 1988. Integrated computer-aided basin modeling applied to analysis of hydrocarbon generation history in a Northern Italian oil field. Org. Geochem. 13, 187–197.

Yalçin, M.N., Littke, R., Sachsenhofer, R.F., 1997. Thermal history of sedimentary basins. In: Welte, D.H., Horsfield, B., Baker, D.R. (Eds.), Petroleum and Basin Evolution. Springer, Berlin, pp. 73–167.